Supporting Information

Ortiz-Castro et al. 10.1073/pnas.1006740108

SI Materials and Methods

Analysis of Growth and Statistical Analysis. Growth of primary roots was registered using a rule. Lateral root number was determined by counting the lateral roots present in the primary root from the tip to the root/stem transition. Fresh weight of plants was determined with an analytical balance (Ohaus Corp.) with a 0.0001-g precision value. For all experiments, the overall data were statistically analyzed in the SPSS 10 software (SPSS). Univariate and multivariate analyses with a Tukey's post hoc test were used for testing differences in growth and root developmental responses in WT and mutant seedlings. Different letters are used to indicate means that differ significantly ($P < 0.05$).

Histochemical Analysis. Transgenic plants that express the *uidA* reporter gene were stained in 0.1% X-Gluc (5-bromo-4-chlorium-3-indolyl, β-D-glucuronide) in phosphate buffer [NaH_2PO_4 and Na_2HPO_4, 0.1 M (pH 7)] with 2 mM potassium ferrocyanide and 2 mM potassium ferricyanide for 12 h at 37 °C (1). Plants were cleared and fixed as previously described (2). The processed roots were included in glass slips and sealed with commercial nail varnish. For each marker line and for each treatment, at least 10 transgenic plants were analyzed.

Microscopy. The *A. thaliana* root system was analyzed with a stereoscopic microscope (Leica MZ6; Leica Microsystems). Total lateral roots were counted at 30× magnification. Primary root meristems were analyzed in semipermanent preparations of cleared roots using a composed microscope (Axiostar Zeiss Plus; Carl Zeiss) at 100× or 400× magnifications. Images were captured with a Sony Cyber-shot DSC-S75 digital camera (Sony) adapted to the microscope and processed with the Zeiss Axio Vision 4AC software (Carl Zeiss).

Propidium Iodide Staining and YFP Detection. For fluorescent staining with propidium iodide (PI), plants were transferred from the growth medium to 10 mg·mL^{-1} of PI solution for 3 min. Seedlings were rinsed in water and mounted in 50% glycerol on microscope slides. The same sample was recorded separately at wavelengths specific to both PI fluorescence with an 568-nm excitation line and emission window of 585–610 nm, and YFP emission with 505- to 550-nm emission filter (488-nm excitation line), using a confocal microscope (Olympus FV1000), after which the two images were merged to produce the final image.

Solvent Extraction, Purification, and Chemical Characterization of Cyclodipeptides from *P. aeruginosa*. A 2.5×10^8 cfu inoculum of WT *P. aeruginosa* and *lasI* mutant strains was placed in 1.5 L Luria Bertani (LB) medium and incubated in a growth cabinet 24 h at 37 °C with shaking for bacterial growth. Cell-free supernatants were prepared by centrifugation (10,000 × *g*, 25 °C for 10 min) in an Eppendorf centrifuge 5810R. The resulting supernatant was extracted twice with ethyl acetate supplied with acetic acid (0.1 mL/L). The extracts were evaporated to dryness (Rotavapor R-210; Buchi) at 60 °C. The residue was redissolved in methanol:acetonitrile (1:1), concentrated, and redissolved to 1 mL in HPLC-grade acetonitrile.

For purification of extracts, 1 mL of extract of ethyl acetate was applied to HPLC system using a C_{18} semipreparative column (Econosil C_{18} 10 U, 250 mm × 22 mm; Alltech). Fractions were eluted with water:acetonitrile, starting with an equilibration step 0:100; followed by a gradient linear up 60:40, with a flow 5 mL·min^{-1} by 40 min; a gradient linear up 90:10, with a flow 5 mL·min^{-1} by 10 min; a gradient linear up 0:100 with a flow 5 mL·min^{-1}; and ending with an equilibration of 15 min with a flow 5 mL·min^{-1}. The deionized water and HPLC-grade acetonitrile were filtrated and degasified. The fractions were collected and concentrated by Freezone 6 lyophilizer (Labconco). The purified fractions were subsequently used for biological activity evaluation and chemical determination.

The purified fractions were analyzed in an Agilent 6850 Series II gas chromatograph equipped with an Agilent MS detector (model 5973) and a 30 m × 0.2 mm × 0.25 mm 5% phenyl methyl siloxane capillary column. Operating conditions used helium as carrier gas, 1 mL/min, with a detector temperature of 300 °C and an injector temperature of 250 °C. The volume of injected sample was 1 μL. The column was held for 3 min at 80 °C and programmed at 6 °C/min to a final temperature of 230 °C for 5 min. A SCAN analysis was used to verify the presence of cycle dipeptides. ^{1}H NMR spectrum of the fractions (1 mg) dissolved in $CDCl_3$ with biology activity was analyzed (Varian Mercury Plus 400 MHz NMR magnet), and the signal assignment was correlated with ^{13}C NMR (Varian Mercury Plus 100 MHz NMR magnet) spectra. The date were analyzed and compared with described compounds and atoms in molecules designed (Fig. S5).

Molecular Docking Analysis of Interactions Between DKPs and TIR1. AutoDock Vina and AutoDock 4.2 software for rigid and flexible (C405, S438, and R489) molecular docking calculations were used. The structure of TIR1 with Aux/IAA7 peptide (PDB ID code 2P1Q) from *A. thaliana* was used as a target. Small molecules used as ligands were cyclo(L-Pro-L-Tyr), cyclo(L-Pro-L-Val), cyclo (L-Pro-L-Phe), and Probe P8 (4). Modeling was carried out with VI EWDD molecular editor (Rome Center for Molecular Design Laboratory). The TIR1 docking site was determined from the TIR1 crystallized structure with IAA, 2,4-D (3), and α-alkyl-IAA (4); a water molecule from the TIR1 auxin-binding site was conserved. A grid box was set to cover the whole docking site (12, 14, 14 grid with a grid spacing of 1.0 Å). One hundred docking runs were performed using the Lamarckian genetic algorithm when AutoDock 4.2 was used. A file comprising all possible conformers was analyzed by AutoDock Tools (5) and figures was generated with PyMOL version 0.99 software (6). The DKP docked conformers were tested according to (*i*) DKP conformers with similar orientation to IAA in the TIR1 model; (*ii*) DKP orientation overlapping with the IAA and 2,4-D binding site in TIRl; (*iii*) DKP orientation selected as present in conformer clusters; (*iv*) DKP conformers with the minimum binding energy to TIR1; and (*v*) DKPs and IAA ability to produce ionic interaction with TIR1 residues involved in molecular binding to polar residue Arg403.

1. Jefferson RA, Kavanagh TA, Bevan MW (1987) GUS fusions: β-glucuronidase as a sensitive and versatile gene fusion marker in higher plants. *EMBO J* 6:3901–3907.
2. Malamy JE, Benfey PN (1997) Organization and cell differentiation in lateral roots of *Arabidopsis thaliana*. *Development* 124:33–44.
3. Tan X, et al. (2007) Mechanism of auxin perception by the TIR1 ubiquitin ligase. *Nature* 446:640–645.
4. Hayashi K, et al. (2008) Small-molecule agonists and antagonists of F-box protein-substrate interactions in auxin perception and signaling. *Proc Natl Acad Sci USA* 105:5632–5637.
5. Sanner MF (1999) Python: A programming language for software integration and development. *J Mol Graph Model* 17:57–61.
6. DeLano WL (2002) The PyMol Molecular Graphics System (DeLano Scientific, Palo Alto, CA).
7. Trott O, Olson AJ; S7 (2010) AutoDock Vina: Improving the speed and accuracy of docking with a new scoring function, efficient optimization, and multithreading. *J Comput Chem* 31:455–461.

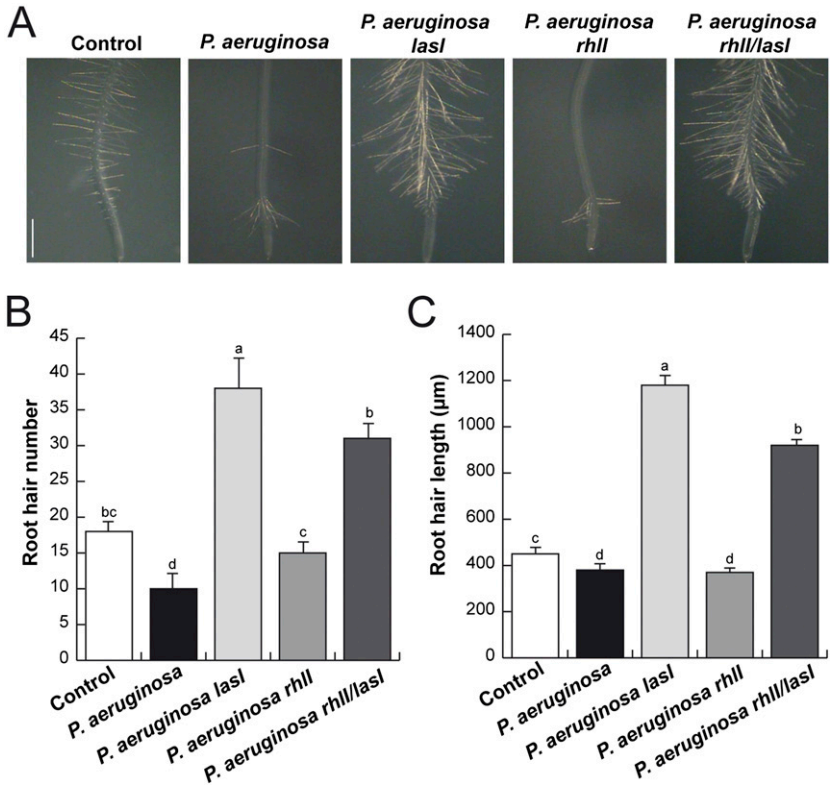

Fig. S1. Effect of cocultivation with *P. aeruginosa* WT and QS mutant strains on root hair development. Four-day-old *A. thaliana* seedlings were cocultivated with WT *P. aeruginosa* or mutants defective on the AHL synthases LasI, RhlI, or RhlI/LasI at a distance of 5 cm from the primary root tip and grown for an additional 8 d. (*A*) Representative photographs of axenically grown *Arabidopsis* seedlings or seedlings cocultivated with WT *P. aeruginosa* and *P. aeruginosa* QS mutants. (Scale bars = 500 μm.) (*B*) Effect of bacterial cocultivation on root hair number or (*C*) root hair length. Data from *B* and *C* show the means ± SD from 30 seedlings. These analyses were repeated three times with similar results. Different letters indicate means statistically different at $P < 0.05$.

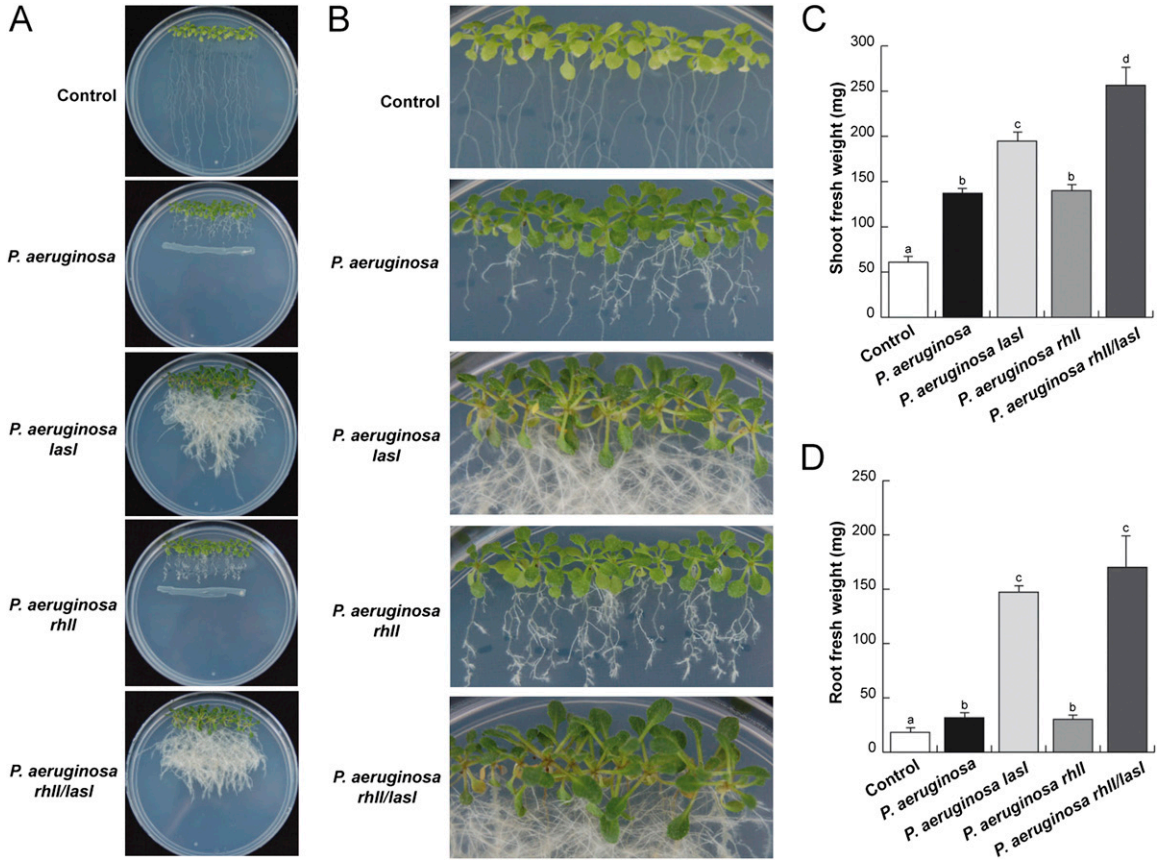

Fig. S2. Effect of cocultivation with *P. aeruginosa* WT and QS mutant strains on plant growth. Four-day-old *A. thaliana* seedlings were cocultivated with WT *P. aeruginosa* or mutants defective on the AHL synthases LasI, RhlI, or RhlI/LasI at a distance of 1 cm from the primary root tip and grown for 12 d. (*A*) representative photographs were taken for plates from each treatment. This experiment includes five different plates per treatment and was repeated three times with similar results. Notice the strong biomass accumulation effect of *P. aeruginosa lasI* and *rhlI/lasI* mutants and the robust induction of lateral roots when the *Arabidopsis* root system establishes physical contact with the bacterial inoculum. (*B*) Close-up photographs from axenically grown plants or plants cocultivated with each bacterial strain. (*C*) Effect of bacterial cocultivation on shoot fresh weight or (*D*) root fresh weight. Data from *C* and *D* show the means ± SD from three groups of 30 seedlings. These analyses were repeated three times with similar results. Different letters indicate means statistically different at $P < 0.05$.

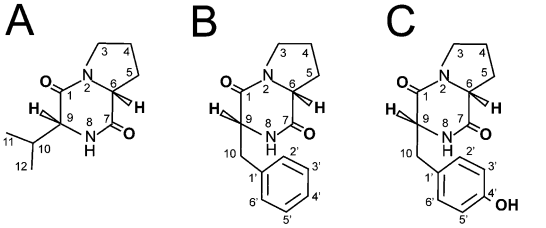

Fig. S3. MS, ^{1}H NMR, and ^{13}C NMR data of DKPs. GC/mass spectrometry, ^{1}H NMR (400 MHz), ^{13}C NMR (100 MHz, $CDCl_3$), spectra δ values data of atom number of (*A*) cyclo(L-Pro-L-Val) [retention time (Rt) = 7.5 min]: mass spectrum shows a molecular ion with mass of 196 (*m/z*), corresponding to molecular formula $C_{10}H_{16}N_2O_2$ [*m/z* (%): 196 (2), 154 (100), 138 (6), 125 (35), 110 (7), 98 (7), 72 (30), 70 (65), 55 (9), 41 (12)]; ^{1}H NMR data: 0.91(3H, d, J = 6.9 Hz CH_3-Val); 1.06 (3H, d, J = 6.9 Hz CH_3-Val); 1.88–2.18 (3H, m, Pro 4-Ha,b, Pro 3-Ha); 2.39 (1H, m, Pro 3-Hb); 2.63 (1H, m, Val H-10); 3.50–3.75 (2H, m, Pro 5-Ha,b); 3.95 (1H, bs, Val H-9); 4.09 (1H, bt, J = 6.9 Hz, Pro H-6); 5.70 (1H, bs, NH); ^{13}C NMR data: 164.8 (C-1), 45.1(C-3), 22.4(C-4), 28.3(C-5), 60.3(C-6), 169.9(C-7), 56.8(C-9), 28.5(C-10), 16(C-11), 19.3 (C-12); (*B*) cyclo(L-Pro-L-Phe) (Rt = 12 min): mass spectrum shows a molecular ion with mass of 244 (*m/z*), corresponding to molecular formula $C_{14}H_{16}N_2O_2$ [*m/z* (%): 244 (58), 153 (48), 125 (100), 120 (20), 103 (6), 91 (42), 70 (40), 55 (5), 41 (6)]; ^{1}H NMR data: 1.85–2.10 (3H, m, Pro 4-Ha,b, Pro 3-Ha); 2.34 (1H, m, Pro 3-Hb); 2.78 (1H, dd, J = 10.6, 14.0 Hz, Phe 10-Ha); 3.55–3.73 (3H, m, Pro 5-Ha,b, Phe 10-Hb); 4.09 (1H, bt, J = 7.3 Hz, Pro H-6); 4.28 (1H, dd, J = 2.2, 10.6 Hz, Phe H-9); 5.62 (1H, bs, NH); 7.22–7.38 (5H, m, Phe); ^{13}C NMR data: 165(C-1), 45.5(C-3), 22.6(C-4), 28.3(C-5), 59.1(C-6), 169.4(C-7), 56.2(C-9), 36.8(C-10), 135.9(C-1′), 129.3(C-3′, C-5′), 129.1 (C-2′, C-6′), 127.6(C-4′); (*C*) cyclo(L-Pro-L-Tyr) (Rt = 7 min): mass spectrum shows a molecular ion with mass of 260 (*m/z*), corresponding to molecular formula $C_{14}H_{16}N_2O_3$ [*m/z* (%): 260 (8), 154 (100), 125 (3), 107 (50), 77 (5), 70 (18), 41 (2)]; ^{1}H NMR data: 1.85–2.10 (3H, m, Pro 4-Ha,b, Pro 3-Ha); 2.4 (1H, m, Pro 3-Hb); 2.74 (1H, dd, J = 10.6, 14.7 Hz, Tyr 10-Ha); 3.40–3.70 (3H, m, Pro 5-Ha,b, Tyr-10-Hb to Tyr 10-Hb); 4.09 (1H, bt, J = 7.7 Hz, Pro H-6); 4.22 (1H, dd, J = 2.2, 10.6 Hz, Tyr H-9); 5.72 (1H, bs, NH); 5.95 (1H, bs, OH); 6.82 (2H, d, J = 8.2 Hz, H-3′,5′ Tyr); 7.07(2H, d, J = 8.2 Hz, H-Tyr Phe); ^{13}C NMR data: 165(C-1), 45.4(C-3), 22.5(C-4), 28.3(C-5), 59.1(C-6), 169.6(C-7), 56.2(C-9), 35.9(C-10), 127.3(C-1′), 116.1(C-3′, C-5′), 130.3(C-2′, C-6′), 155.3(C-4′).

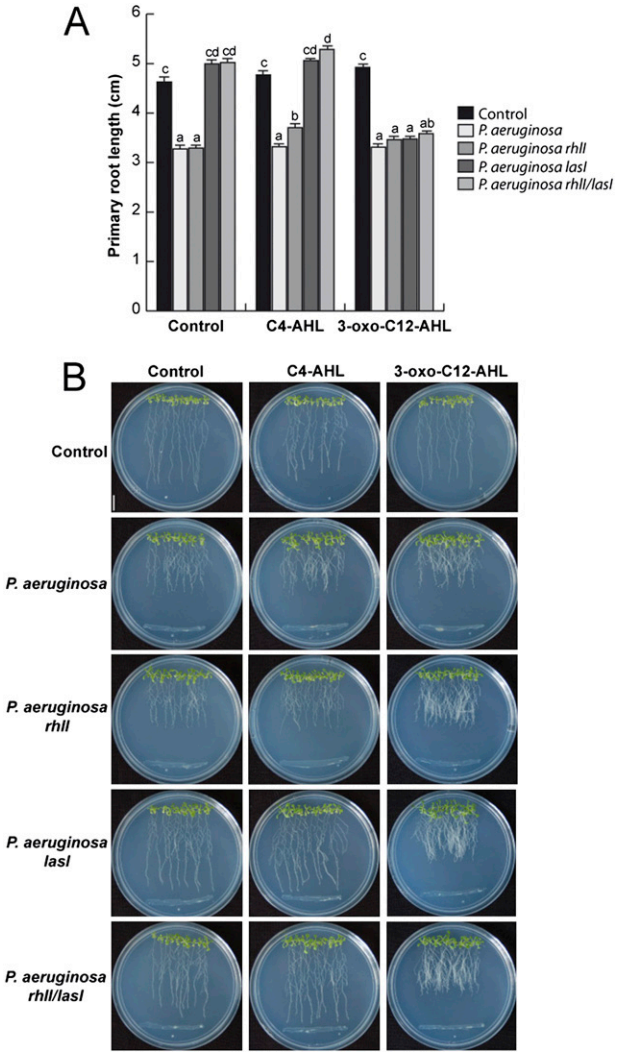

Fig. S4. Chemical complementation of *P. aeruginosa* QS mutants. *A. thaliana* seedlings were germinated and grown on 0.2× MS agar medium supplemented with or without 10 μM C4-AHL or 3-oxo-C12-AHL. Four-day-old seedlings were cocultivated with WT *P. aeruginosa* or mutants defective on the AHL synthases LasI, RhlI, or RhlI/LasI at a distance of 5 cm from primary root tip and grown for an additional 8 d. Data points shown in *A* represent mean primary root length ± SD (n = 30). (*B*) Representative photographs of plants from the different treatments. (Scale bars = 1 cm.) These analyses were repeated three times with similar results. Different letters indicate means statistically different at $P < 0.05$.

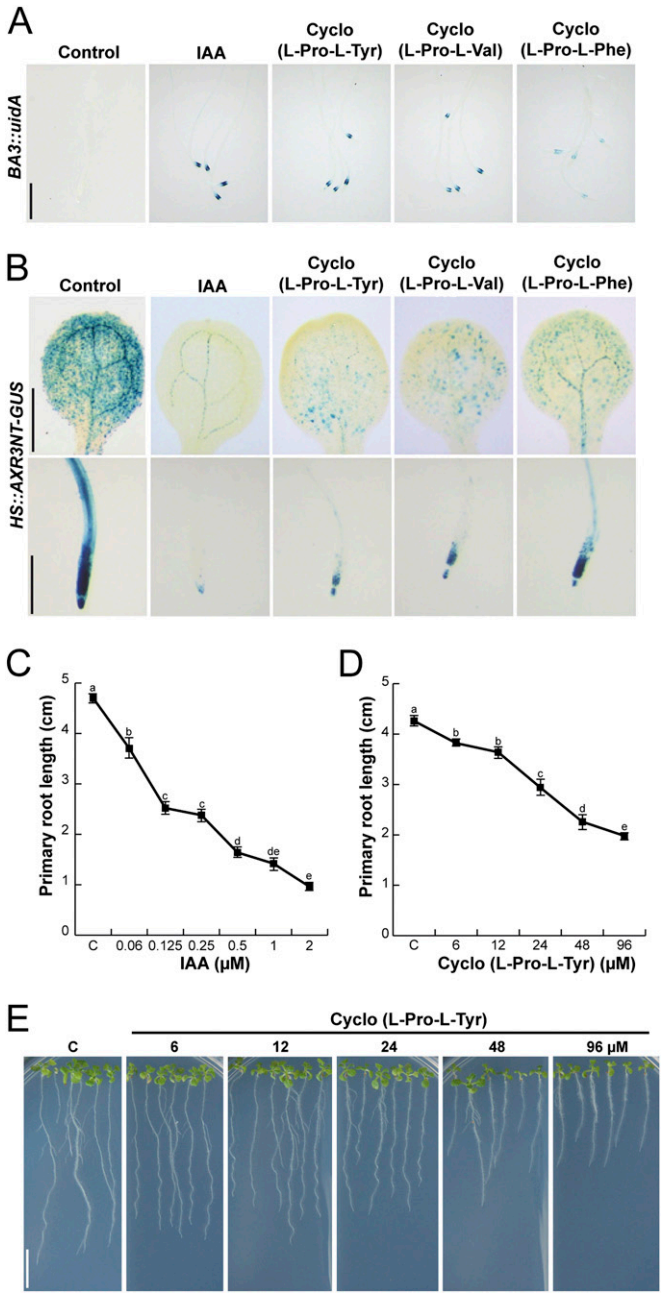

Fig. S5. Effects of IAA and bacterial DKPs on auxin-regulated gene expression and primary root growth. (*A*) *BA3:uidA* auxin-regulated gene expression. Six-day-old *BA3:uidA* seedlings were transferred for 12 h of β-glucuronidase staining to 24-well plates containing 2 mL of liquid 0.2× MS medium supplied with 3 μM IAA or 30 μM DKP. (*B*) Effect of DKPs on AXR3 degradation. Six-day-old *HS:AXR3NT-GUS* seedlings grown on 0.2× MS medium were heat shocked for 2 h a 37 °C and then transferred for 60 min to 0.2× MS liquid medium containing 3 μM IAA or 30 μM DKPs. Plants were stained for β-glucuronidase activity and cleared to show gene expression. Photographs show representative individuals from at least 10 stained plants. (Scale bars = 500 μm.) (*C*–*E*) Effects of IAA and cyclo(L-Pro-L-Tyr) on primary root growth. WT *A. thaliana* (Col-0) seedlings were germinated and grown for 8 d on 0.2× MS agar medium supplemented with the indicated concentrations of IAA (*C*) or cyclo(L-Pro-L-Tyr) (*D*) and primary root length recorded for 15 seedlings. (*E*) Representative photographs of *Arabidopsis* seedlings treated with cyclo(L-Pro-L-Tyr). Data points show the mean primary root length ± SD. Different letters indicate means that differ statistically at $P < 0.05$. (Scale bars = 1 cm.)

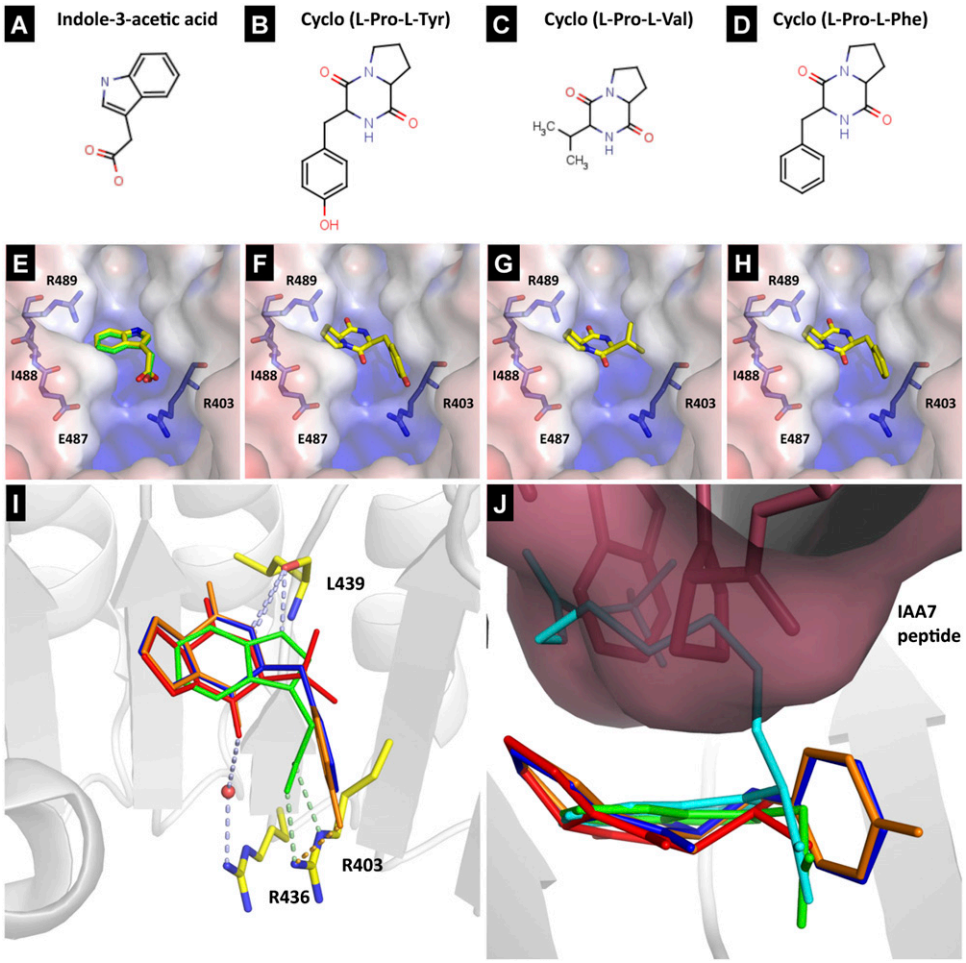

Fig. S6. Modeling of *P. aeruginosa* DKPs in the TIR1-IAA auxin receptor of *A. thaliana* using the software AutoDock Vina and Autodock 4.2 (2). Chemical structures of IAA and DKPs from *P. aeruginosa*: (*A*) IAA, (*B*) cyclo(L-Pro-L-Tyr), (*C*) cyclo(L-Pro-L-Val), (*D*) cyclo(L-Pro-L-Phe), and (*E–H*) structural position of IAA and DKPs, respectively, in the auxin-binding cavity of TIR1. Residues involved in pocket formation (E487, I488, and R489) and residue (R403) involved in the interaction with auxin carboxyl group are indicated in surface representation. (*I*) A close-up view of the IAA and DKPs superposition in the auxin-binding site of TIR1. IAA (green), cyclo(L-Pro-L-Tyr) (orange), cyclo(L-Pro-L-Val) (red), cyclo(L-Pro-L-Phe) (blue), and a water molecule (red sphere). Interacting residues of IAA and DKPs with TIR1 are indicated by dashed lines. (*J*) Modeling of IAA, DKPs, and Aux/IAA7 degron peptide superimposed in the crystal structure of the TIR1 auxin-binding site. IAA and DKPs are shown as in *I*, antiauxinic molecule α-butyl-indole-3-acetic acid (probe 8) (2) is shown as light blue. The DKP-TIR1 binding energy obtained was near the range of redocked auxins (IAA = −8.1 kcal/mol; 2,4-D = −7.2 kcal/mol; cyclo(L-Pro-L-Tyr) = −3.7 kcal/mol, cyclo(L-Pro-L-Val) = −5.3 kcal/mol, and cyclo(L-Pro-L-Phe) = −4.0 kcal/mol). Also, the dimension (5.5 Å) of *P. aeruginosa* DKPs identified was similar to IAA (4.66 Å), NAA (4.86 Å), and 2,4-D (5.27 Å).

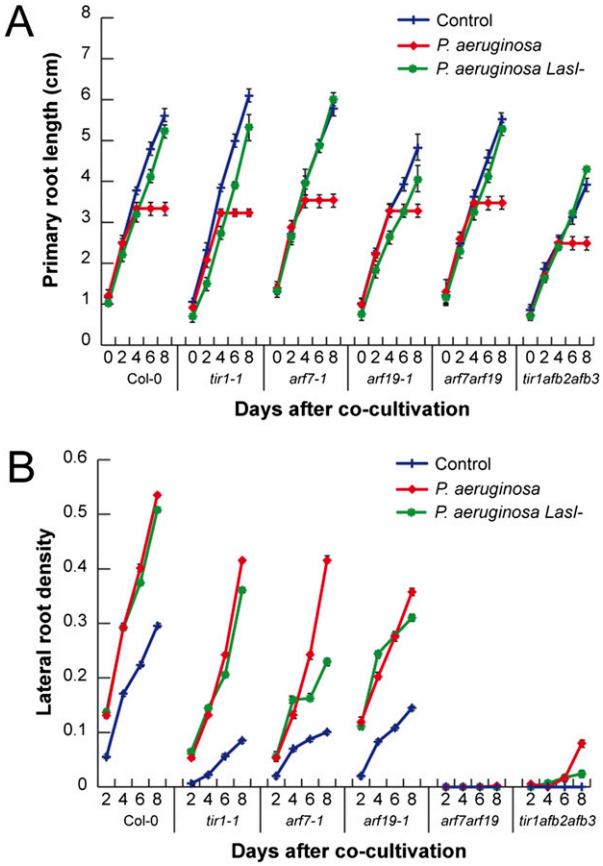

Fig. S7. Effect of cocultivation with *P. aeruginosa* WT and QS-related mutant strains in RSA development in *Arabidopsis* WT and auxin-related mutant lines. Four-day-old *A. thaliana* WT and *tir1-1*, *arf7-1*, *arf19-1*, *arf7arf19*, and *tir1afb2afb3* mutant lines were inoculated with WT *P. aeruginosa* or with mutants defective on the AHL synthases LasI at a distance of 5 cm from the primary root tip and grown for an additional 8 d. The effect of bacterial cocultivation on primary root length (*A*) or lateral root density (*B*) was monitored every 2 d. Day 0 indicates the length reached by the primary root at the moment of bacterial inoculation. Data points show the mean ± SD. The experiment was repeated twice with similar results.

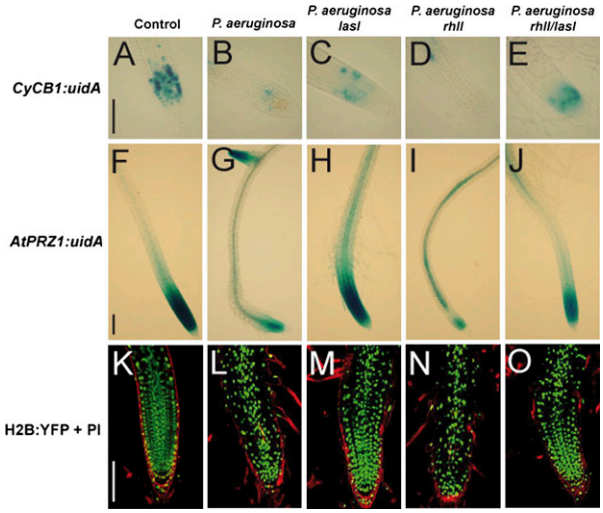

Fig. S8. Effect of cocultivation with *P. aeruginosa* WT and QS mutant strains on cell division and meristem cell viability. Four-day-old *A. thaliana* seedlings expressing the *CyCB1:uidA*, *AtPRZ1:uidA*, or *AtHistH2B:YFP* markers were cocultivated with WT *P. aeruginosa* or mutants defective on the AHL synthases LasI, RhlI, or RhlI/LasI at a distance of 1 cm from primary root tip and grown for an additional 6 d. (*A–J*) Plants were stained for GUS activity and cleared to show gene expression. (*K–O*) Transgenic *Arabidopsis* seedlings expressing the *AtHistH2B:YFP* marker were stained with PI to determine cell structure and viability. Photographs show representative individuals from at least 20 stained plants. The experiment was replicated twice with similar results. (Scale bar = 100 μm.)

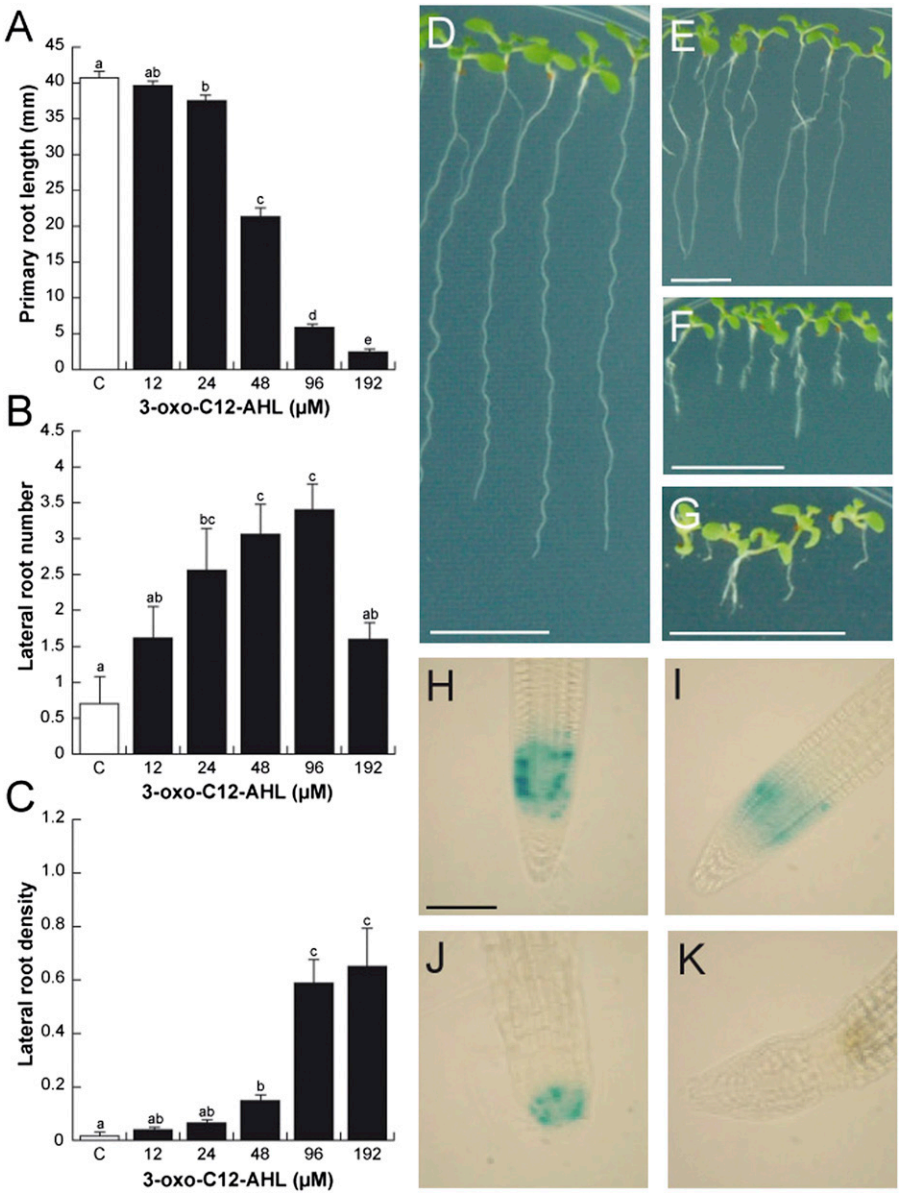

Fig. S9. Effects of 3-oxo-C12-AHL on root system architecture and cell division marker expression in *Arabidopsis*. *A. thaliana* (Col-0) seedlings were germinated and grown for 10 d on 0.2× MS agar medium supplemented with the indicated concentrations of 3-oxo-C12-AHL, and primary root length (*A*), lateral root number (*B*), and lateral root density (*C*) were recorded for 30 seedlings. Representative photographs of *Arabidopsis* seedlings treated with solvent (*D*) or 48 μM (*E*), 96 μM (*F*), and 192 μM (*G*) of 3-oxo-C12-AHL. Data points in *A*–*C* show the mean ± SD from 30 seedlings. Different letters indicate means that differ statistically at $P < 0.05$. (*H*–*K*) Transgenic *Arabidopsis* seedlings expressing the *CyCB1:uidA* marker were grown for 10 d in medium with the solvent—48, 96, or 192 μM of 3-oxo-C12-AHL, respectively. Plants were stained for GUS activity and cleared to show gene expression. Photographs show representative individuals from at least 20 stained plants. The experiment was replicated twice with similar results. (Scale bars: *D*–*G*, 1 cm; *H*, 100 μm.)

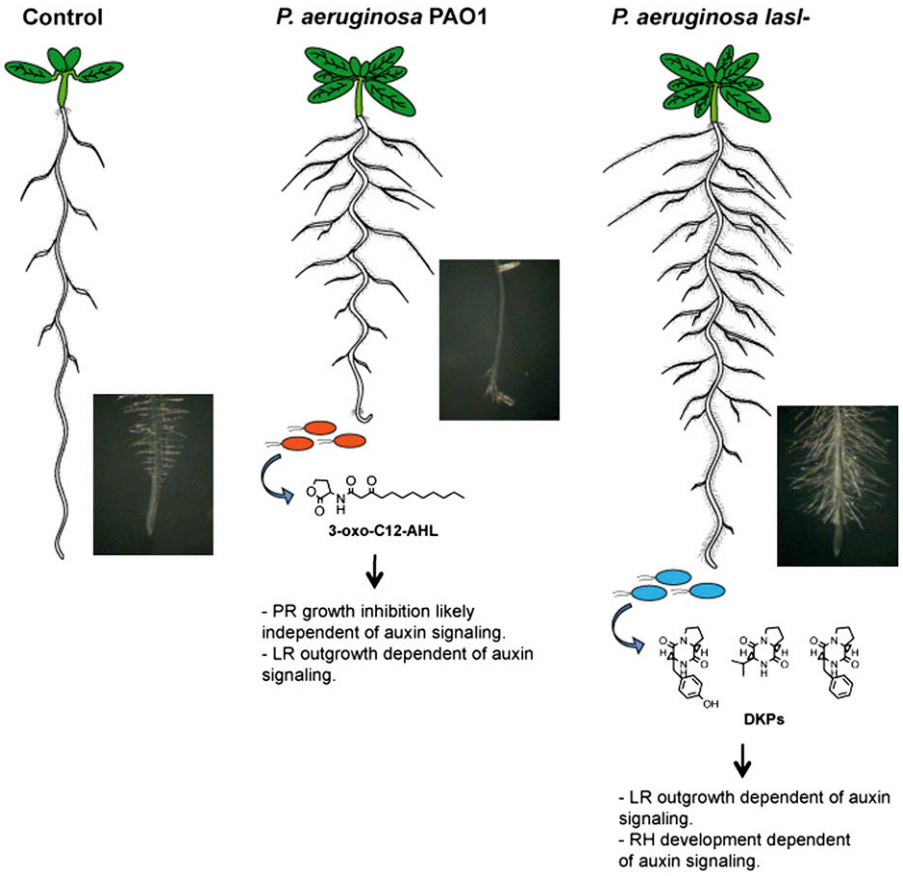

Fig. S10. Root architectural responses of *Arabidopsis* to WT *P. aeruginosa* and QS-related mutants.